JOURNAL OF CATALYSIS **177,** 325–334 (1998)
ARTICLE NO. CA982095

Direct Evidence of Active Surface Reconstruction during Oxidative Dehydrogenation of Propane over VMgO Catalyst

A. Pantazidis,* A. Burrows,† C. J. Kiely,† and C. Mirodatos*,[1]

*Institut de Recherches sur la Catalyse, C.N.R.S., 2, avenue Albert Einstein, F-69626 Villeurbanne Cédex, France; and †Department of Materials Science and Engineering, The University of Liverpool, Liverpool, Merseyside, L69 3BX, United Kingdom

Received November 3, 1997; revised March 17, 1998; accepted March 26, 1998

This paper presents a thorough investigation of an optimised VMgO catalyst (14 wt% V) for the oxidative dehydrogenation of propane, carried out in order to elucidate the nature and behaviour of the active surface. The catalyst morphology and the surface composition are studied by means of HREM, XPS, UV-vis, XRD, and *in-situ* electrical conductivity techniques, as a function of the gaseous environments of the catalyst. The active surface is shown to be essentially a monolayer of amorphous VO_4^{3-} units scattered over the magnesia as isolated and polymeric species. These surface vanadia units are found to stabilise an unusual polar (111) orientation of MgO up to temperatures of 800°C. A direct and outstanding evidence of a totally reversible phenomenon of order/disorder restructuration of this V overlayer is provided in conjunction with the redox state of the surface depending on the properties of the surrounding atmosphere (reductive or oxidative). These fast surface phenomena are assumed to determine the elementary steps of propane activation within the overall ODHP process.

1. INTRODUCTION

In recent years, the dynamics of catalytic surfaces under reaction conditions such as reconstruction or segregation have been investigated extensively on metal catalysts, mostly by means of surface science techniques (1). In the case of real oxide catalysts, such an approach faces the extreme difficulty of direct *in-situ* investigation on surfaces highly sensitive to the surrounding atmosphere (2). Thus, for oxidation reactions which proceed via the Mars–van Krevelen mechanism, the continuous change in the degree of oxidation/reduction of the surface, the migration of lattice oxygen/vacancies throughout the bulk oxide may result in deep changes in the surface structure, depending on the operating conditions. As a result, the precise nature and concentration of the active sites remains most often a matter of speculation. The oxidative dehydrogenation of propane (ODHP) over vanadium-magnesium oxides is a typical example of a catalytic oxidation reaction for which a direct observation of the reacting surface has never been reported. This contrasts with the large effort of research on the catalyst, the reaction mechanism, and the kinetics within the challenging topic of light alkane dehydrogenation (3–8).

Recent studies (9–11) on the ODHP reaction revealed that the good catalytic performances generally obtained over VMgO catalysts could be optimised for low V contents and high calcination temperature. Thus, the highest propene yields were obtained for a catalyst containing 14 wt% of vanadium after calcination at 800°C. Selectivity to propene was shown to have little dependence on the surface composition and structure, while intrinsic activity presented a high structure sensitivity (9). Several characterization data (9–11) suggested that the optimised active surface could not simply be related to a well-defined crystallographic phase or to some synergetic effect between two phases present in significant amounts: MgO and Mg orthovanadate, as often postulated in the literature (3, 4, 8). It was proposed instead from preliminary characterisation data that the active and selective phase would be formed of dispersed amorphous vanadium units, this assumption being consistent with the low V content of the optimised catalyst.

In order to further elucidate the exact nature and behaviour of the active surface under ODHP reaction conditions, we have thoroughly investigated the morphology and the structure of the optimised catalyst, as well as the influence of various gaseous environments on the state of its surface. This study was carried out by means of *ex-situ* (HREM, XPS, UV-vis, and XRD) and *in-situ* (electrical conductivity) techniques. An advanced quantification of the sites concentration by means of kinetic (isotopic transient and steady-state) and modelling methods will be presented in a further publication (12).

2. EXPERIMENTAL

2.1. Catalyst Preparation

$Mg(OH)_2$ was first precipitated from a magnesium nitrate solution ($Mg(NO_3)_2 \cdot 6H_2O$, Prolabo, 0.286 *M*) by a

[1] Corresponding author. E-mail: mirodato@catalyse.univ-lyon1.fr.

0021-9517/98 $25.00

potassium hydroxide solution (KOH, Prolabo, 0.343 *M*) using intense agitation. The precipitate was separated from the solution by centrifugation and then dried in vacuo at 100°C overnight. It was then crushed, washed, and centrifuged repeatedly (4–5 times). The solid was dried again and was immediately used in order to avoid further carbonate formation. The $Mg(OH)_2$ material thus obtained was added to a slightly basic hot aqueous (1 vol% of NH_4OH) solution of ammonium metavanadate (NH_4VO_3, Aldrich). The suspension was evaporated to dryness and dried overnight at 120°C. The resulting solid was crushed and calcined under an O_2/He flow ($P(O_2) = 4.0$ kPa) at 550°C for 6 h and then at 800°C (6 h). It was sieved to particles with a diameter ranging from 0.1 to 0.2 mm before use, unless specified. The vanadium content was 13.5 wt% as determined by chemical analysis. The catalyst is referred to as 14V/VMgO.

2.2. Catalytic Treatments

The fresh sample (referred to as "FRESH") was tested for the ODHP in a fixed bed reactor at 500°C under atmospheric pressure. The reaction feed consisted typically of a C_3H_8/O_2/He mixture = 1.32/0.66/98.02% with a total flow rate of 60 ml/min. The material obtained after a 50-h run is referred to as the "USED" sample. Reduction–reoxidation (redox) sequences were also carried out at 500°C under the following mixtures: (i) O_2/He = 2.0/98.0%; (ii) C_3H_8/He = 2.4/97.6% ("USED-P" sample); and (iii) again O_2/He = 2.0/98.0% ("REOX" sample).

2.3. Catalysts Characterization

Surface area. Surface areas were measured by nitrogen adsorption, according to the BET method. The samples were analysed in a BET quartz cell designed for *in-situ* treatments such as calcination and ODHP reaction.

X-ray diffraction. Samples were analysed on a Phillips PW 1710 diffractometer with Cu $K\alpha$ radiation under standard acquisition conditions. A JCPDS-ICDD (1990–1991) standard spectra software was used to identify the different phases present in the solids.

X-ray photoelectron spectroscopy. XPS measurements were carried out on a VG-model ESCA III spectrometer. The exciting radiation was Mg$K\alpha$ (1253.6 eV). The binding energies were calibrated with respect to the C 1s energy at 284.9 eV corresponding to the pollution carbon. The samples were pretreated in a heated reaction chamber under flowing gases before being transferred into the XPS chamber. The 14V/VMgO catalyst was analyzed (i) after pretreatment under a O_2/He mixture = 2.0/98.0% at 560°C for 30 min and (ii) after a treatment under the reacting mixture C_3H_8/O_2/He = 7.1/3.7/89.2% at 560°C for 30 min.

Electrical conductivity. The catalyst powder was slightly compressed between two Pt electrodes. The electrical resistance was measured with an ohm-meter (Kontron, Model DMM 4021) for $1 \le R \le 2 \times 10^6$ ohm and with a teraohm-meter (Guildline Instruments Model 9520) for $10^6 \le R \le 10^{14}$ ohm. The electrical conductivity σ (ohm^{-1} cm^{-1}) was determined using the formula: $\sigma = (R * S/h)^{-1}$, where R is the measured electrical resistance (ohm), S is the cross sectional area of the electrodes (cm^2), and h is the catalyst bed thickness (cm). The partial pressure of oxygen and temperature were varied in order to check the nature, *n*- or *p*-type, of the electrical conductivity (13). Reduction–reoxidation (redox) sequences were carried out at 500°C in the presence of propane ($P_{C_3H_8} = 2.4$ kPa), then of reaction mixture ($P_{C_3H_8} = 2.4$ kPa, $P_{O_2} = 2.0$ kPa), then of oxygen ($P_{O_2} = 2.0$ kPa), refered to as USED-P, USED, and REOX steps, respectively. Steady state was attained between each step.

Ultraviolet diffuse reflectance spectroscopy (UV-vis DR). DR spectra in the UV-visible region (190–800 nm) were collected with a Perkin-Elmer Lambda 9 spectrometer. The samples were pressed into a disk and the spectra were recorded in air at room temperature. MgO was taken as a reference material.

High resolution electron microscopy (HREM). The "FRESH," "USED," "USED-P," and "REOX" samples were examined in a JEOL 2000EX high-resolution electron microscope fitted with a LaB_5 source operating at 200 kV. Catalyst powders were ground gently using an agate mortar and pestle in the presence of ethanol. One or two drops of the resulting slurry were deposited onto a 3.05-mm holey carbon-coated copper mesh grid. Additional TEM investigation was performed on a JEOL JEM 2010 fitted with an energy dispersive X-ray (EDX) spectrometer (Link-Isis), allowing chemical micro analysis.

3. RESULTS

3.1. Structural and Surface Properties

BET measurements carried out on the "FRESH" and the "USED" samples indicated that no significant change in surface area occurred during the ODHP reaction (43 and 41 m^2 g^{-1}, respectively, Table 1).

Figure 1 shows the XRD pattern obtained from the "FRESH" sample. A quite similar pattern was obtained for the "USED" sample. They clearly show the prominent presence of MgO coexisting with a minor phase of well-crystallised orthovanadate $Mg_3V_2O_8$. Traces of other vanadate structures (pyro or meta) cannot be excluded.

Table 1 reports the V/Mg atomic ratios obtained from chemical analysis and the V/Mg, O/V, and O/Mg surface atomic ratios calculated from the Mg_{2p}, O_{1s}, and $V_{2p\ 3/2}$ XPS spectra. The XPS Mg/V surface atomic ratio (about 12.5)

TABLE 1

Surface Area and Composition Analysis of the 14V/VMgO Catalyst (Pantazidis (11))

Technique	Property	"FRESH"	"USED"
BET	S_{BET} (m^2/g)	43	41
XPS	Mg/V (atomic)	12.3	12.6
	O/V (atomic)	13.4	14.2
	O/Mg (atomic)	1.09	1.13
Chemical analysis	Mg/V (atomic)	6.6	6.8

was found to be much larger than the theoretical ratio of the orthovanadate phase (Mg/V = 1.5). This demonstrates that the catalyst surface must be considered mainly as magnesia supporting vanadium atoms rather than a stoichiometric vanadate. However, the smaller Mg/V overall ratio (6.6 from chemical analysis) is consistent with the XRD observation that some bulk vanadate crystals coexist with the material supported on magnesia. The slight increase in the Mg/V and O/V XPS ratios observed for the "USED" sample could arise from some surface enrichment in MgO (or V depletion) and/or from a vanadium phase sintering which would occur under the ODHP reaction conditions.

The $V_{2p\ 3/2}$ XPS spectra were decomposed into two peaks at 517.3 and 515.9 eV, which corresponded to values generally attributed to V^{5+} and V^{4+} ions, respectively (8, 14). The surface V^{4+}/V^{5+} atomic ratio is estimated to be 0.18 and 0.26 before and after reaction, respectively. Although these values are related to the state of the catalyst under the vacuum conditions of the XPS analysis, they indicate that the reaction tends to reduce the surface. Recent *in-situ* EXAFS study carried out on a similar 14V/VMgO sample in propane rich (1% C_3H_8, 0.1% O_2) feeds showed that the presence of V^{3+} is also likely under highly reducing atmosphere (15).

By measuring the electrical conductivity as a function of the partial pressure of oxygen and temperature, the 14V/VMgO sample was found to behave as a semiconductor, with σ varying exponentially with T, according to $\sigma = \sigma_O \exp(-E_c/RT)$. E_c, the activation energy of conduction, was found to be 135 kJ/mol., a value close to the one reported for unpromoted magnesia (10). The slope $(1/n)$ of the isotherm $\log \sigma = f(\log P_{O_2})$ was found to be $-1/19$. This negative value demonstrates the n-type character of the semiconductor. However, the physical meaning of the $1/n$ value of the isotherm slope is not obvious. Values of n close to 6 correspond to the model of doubly ionised anionic vacancies ($V_{O^{2-}}^{2+}$ or □) (13). Higher values ($n > 10$), as observed for the present VMgO sample, calcined at 800°C may imply the contribution of other types of surface defects or adspecies besides the above anionic vacancies (13).

In-situ electrical conductivity experiments were performed during reduction–reoxidation (redox) sequences at 500°C (Fig. 2). At time 0, the catalyst was under an oxygen atmosphere at 500°C ("FRESH" sample). As pure propane was introduced (point A: "USED-P" sample), the n-type electrical conductivity (σ) increased by several orders of magnitude, indicating a substantial release of free electrons

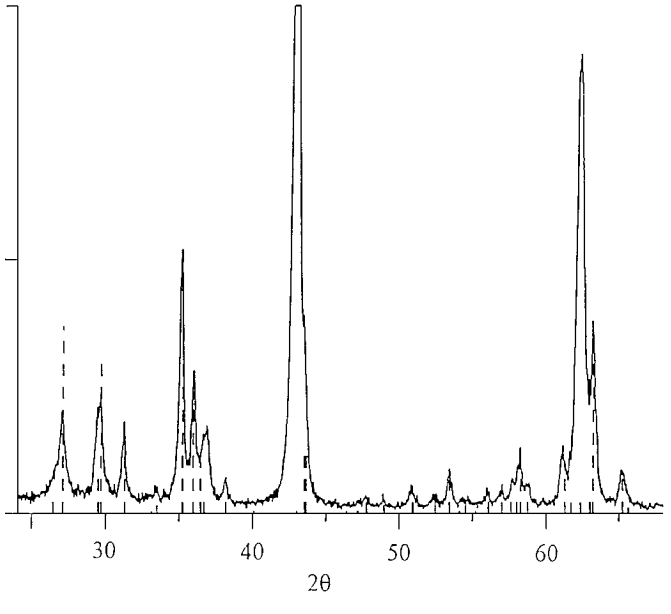

FIG. 1. XRD spectrum for the 14V/VMgO catalyst FRESH or USED (both spectra are similar). In dotted bars, the JCPDS-ICDD data corresponding to $Mg_3V_2O_8$. The three nonindexed bands (for the sake of clarity) at $2\theta = 37.0$, 42.9, and 62.4 correspond exactly to the MgO structure with the relative intensity 4, 100, and 39, respectively (powder diffraction file 45-0946, JCPDS-ICDD).

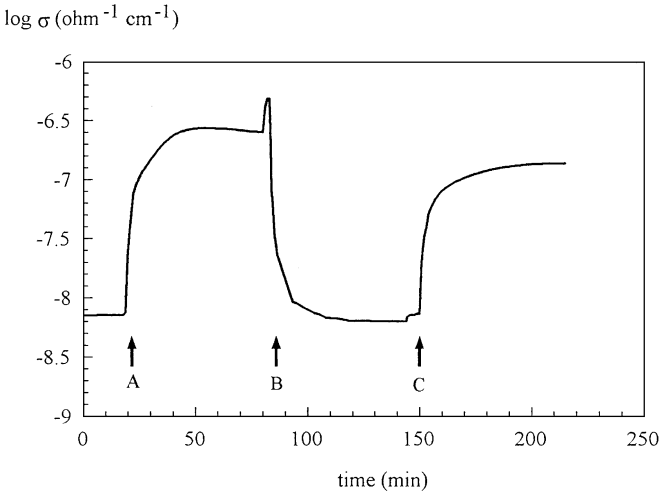

FIG. 2. Variation of the electrical conductivity σ during redox sequences at 500°C on the 14V/VMgO catalyst calcined at 800°C; initial atmosphere: oxygen; (A) propane; (B) vacuum, then oxygen; and (C) ODHP reaction mixture.

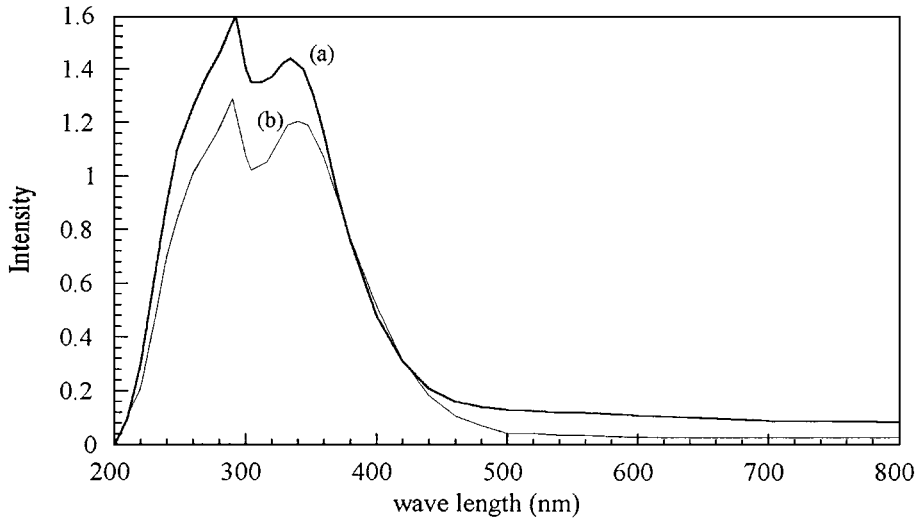

FIG. 3. UV-vis spectra obtained with the "FRESH" (a) and the "USED" (b) 14V/VMgO samples.

available for conduction, which corresponds to a partial reduction of the catalyst. When reintroducing oxygen (point B: "REOX" sample) the electrical conductivity dropped back to the initial value ($\log \sigma = -8.15$), demonstrating the reversibility of the reduction process. When the reacting mixture oxygen/propane was introduced (point C: "USED" sample), the electrical conductivity was lower than in the presence of pure propane. The catalyst was therefore reduced to a lesser extent under ODHP reaction conditions than in the presence of pure propane.

Figure 3 shows the UV-vis DR spectra obtained on "FRESH" (a) and "USED" (b) samples. A strong absorption was observed for both samples between ca 250 and 400 nm. This DR absorption range is characteristic of charge transfer occurring between O^{2-} and V^{5+} ions in tetrahedral coordination (6, 16). Similar charge transfer for vanadium ions in octahedral coordination would have been observed in the 400–500-nm range. More precisely, two main bands of close intensity were observed at 250–290 nm and 300–350 nm. According to Corma *et al.* (6), these bands can be associated to isolated and distorted (interacting with other V ions) VO_4^{2-} tetrahedra, respectively. This assignment is consistent with the preferential development of the DR absorption at 300–350 nm when increasing the V content in the V/VMgO catalyst (unpublished results). Although no direct information is available from the absolute band intensity (no precise calibration of the signal), the relative band intensity may inform us about the distribution of the different types of VO_4^{2-} species. The deconvolution of the energy spectra (cm^{-1}) into bands of Gaussian shape showed that the relative concentration of the distorted tetrahedra tended to slightly increase at the expense of the isolated monomeric species after ODHP reaction. The above trend would indicate some polymerisation effect between isolated species, induced by the reaction. Note, however, that the UV-vis DR signal reflects both surface and bulk V-O charge transfer phenomena. This may minimize specific surface effects since the bulk vanadate crystallites do not undergo structural changes after ODHP reaction, as indicated by XRD (Fig. 1).

3.2. Particle Morphology before Catalytic Treatment

Figure 4a is a low-magnification micrograph of the "FRESH" catalyst material which shows a bimodal size distribution of particles, with (i) numerous small 20–40-nm particles (labelled A) and (ii) large and much less numerous particles (labelled B) ranging from 110 to 180 nm. HREM and EDX analysis (Table 2) show that the small A particles are platelets of MgO loaded with a very small amount of V atoms (mean atomic ratio V/Mg = 1/45), whilst the large B particles correspond to discrete VMgO phases with a mean atomic ratio of V/Mg = 2/3. The latter ratio perfectly confirms the XRD observation of the orthovanadate phase $Mg_3V_2O_8$. Figure 4b shows the same area of material after approximately 45-s exposure to the electron beam. The VMgO phases (B) are unstable and tend to become amorphous rapidly under the influence of the beam. On the other hand, the MgO platelets (A) remain crystalline but undergo a rather severe reconstruction after a few minutes irradiation, as shown in Fig. 4c. The MgO particles develop numerous {100}-type facets as opposed to the rather smooth

TABLE 2

EDX Analysis on the "FRESH" 14V/VMgO Sample

	Small particles (A)	Large particles (B)
V wt%	1–5	20–30
V/Mg atomic ratio	1/45	2/3

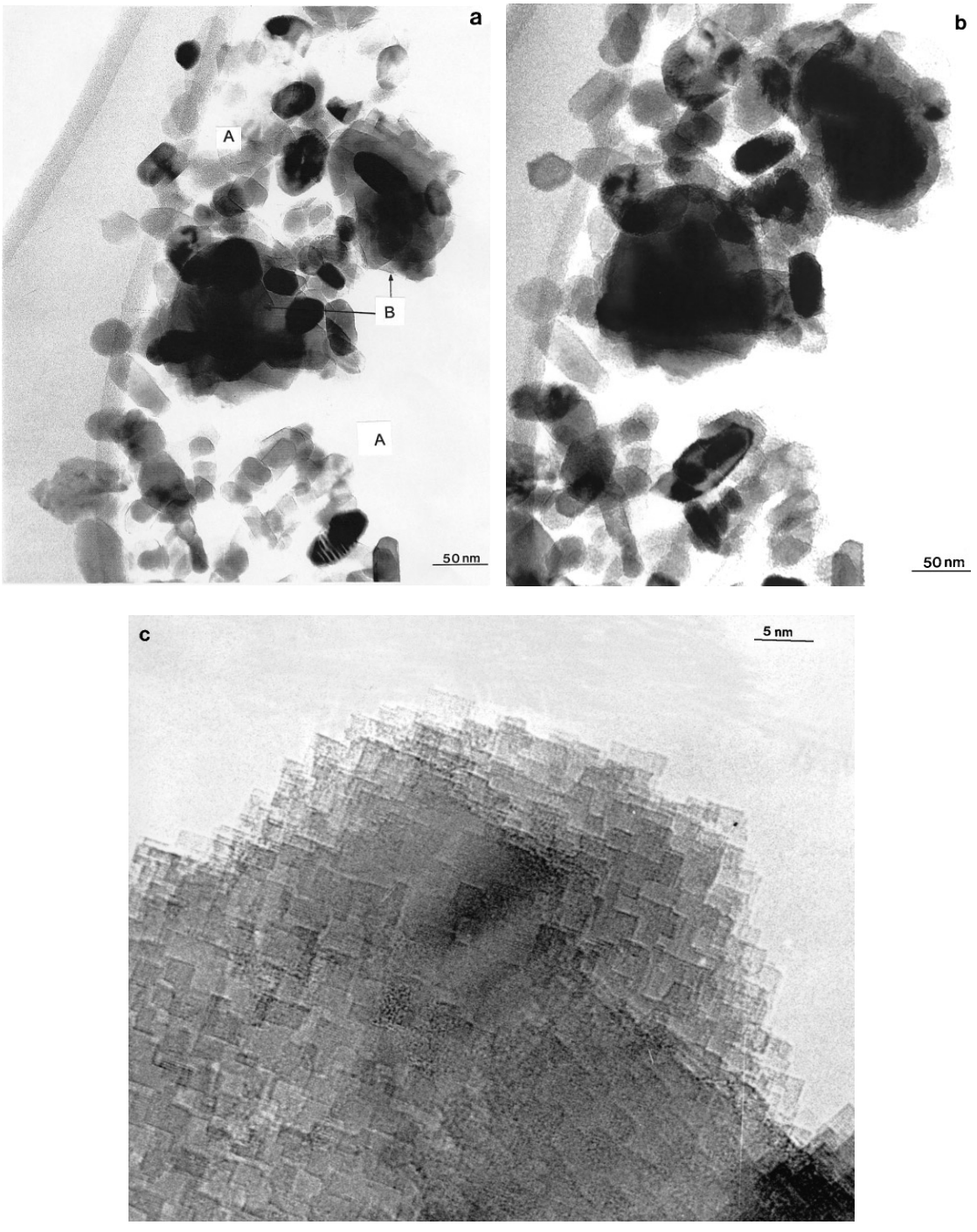

FIG. 4. Low magnification micrographs after few seconds (a) and after approximately 45 s exposure to the electron beam (b) of the "FRESH" 14V/VMgO sample. High magnification micrograph of the MgO platelets after few minutes irradiation (c).

surfaces and sometimes pseudo-hexagonal morphology exhibited by the MgO in Fig. 4a.

When the large VMgO particles were observed at high magnification, it became possible to identify the bulk phases present by careful measurement of lattice fringe spacing and intersection angles. Most of the particles were found to correspond to the magnesium orthovanadate ($Mg_3V_2O_8$) phase, again in full agreement with the XRD measurements. An example is shown in Fig. 5a which corresponds to the [100] zone axis of $Mg_3V_2O_8$ in which the $(0\bar{2}\bar{1})$, $(02\bar{1})$, and (002) lattice planes are resolved. About one in 20 of the larger VMgO particles observed were found to match to the

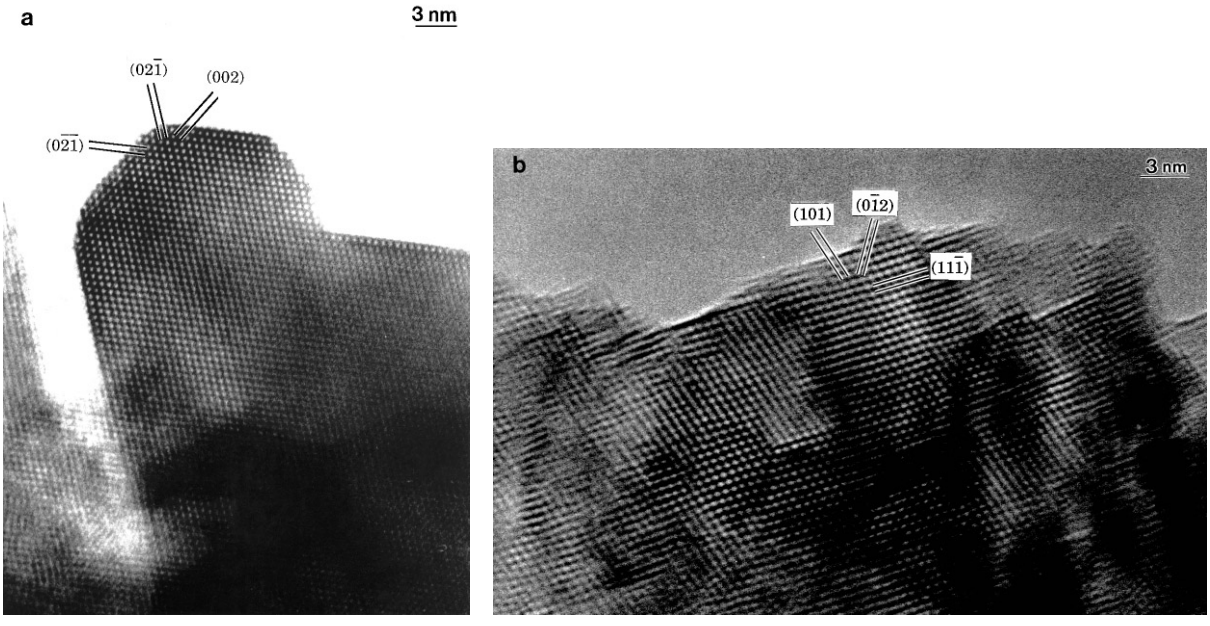

FIG. 5. High magnification micrographs of the large particles of the "FRESH" 14V/VMgO sample: [100] zone axis of $Mg_3V_2O_8$ in which the $(0\bar{2}\bar{1})$, $(02\bar{1})$, and (002) lattice planes are resolved (a); $[\bar{1}2\bar{1}]$ projection of $Mg_2V_2O_7$ (b).

magnesium pyrovanadate ($Mg_2V_2O_7$) phase. An example is shown in Fig. 5b, where the $[\bar{1}2\bar{1}]$ projection of $Mg_2V_2O_7$ is presented. This latter phase was not detected by XRD analysis which is not surprising, considering its rather rare occurrence.

Figure 6 shows an edge-on HREM micrograph, taken under low-dose imaging conditions of an MgO platelet. The viewing direction corresponds to [110] in which two sets of {111}-type fringes and a set of (002) fringes are resolved. These are indexed on the micrograph and it is immediately apparent that one set of {111} fringes run parallel to the MgO platelet surface. This unequivocally demonstrates that the platelets are terminated by energetically unfavourable polar {111}-type planes rather than the usual nonpolar {100}-type. Both of these types of surface termination are shown schematically in Fig. 7. The (111) facet termination of the MgO platelets has recently been shown to arise initially from the structural transformation that occurs when the parent brucite ($Mg(OH)_2$) crystallite thermally decomposes to form MgO (17). This (111) orientation

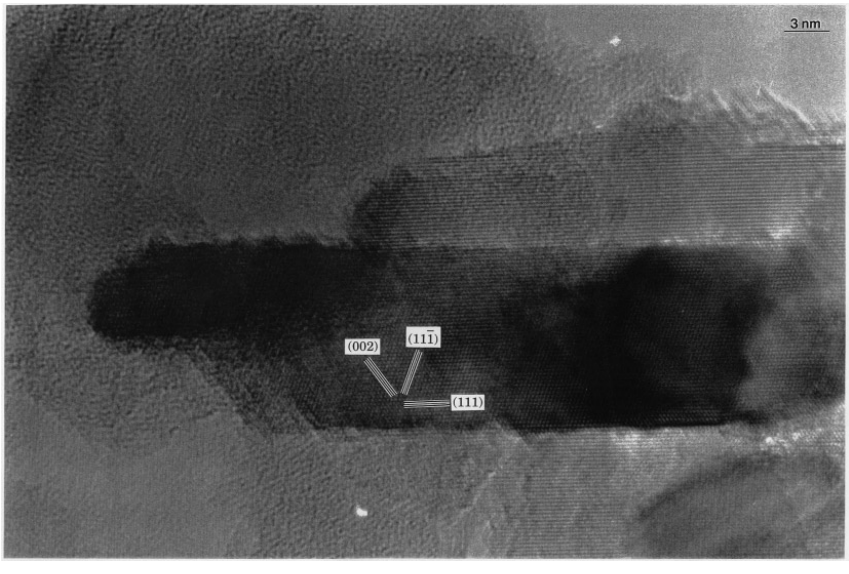

FIG. 6. Edge-on HREM micrograph, taken under low-dose imaging conditions, of an MgO platelet of the "FRESH" 14V/VMgO sample.

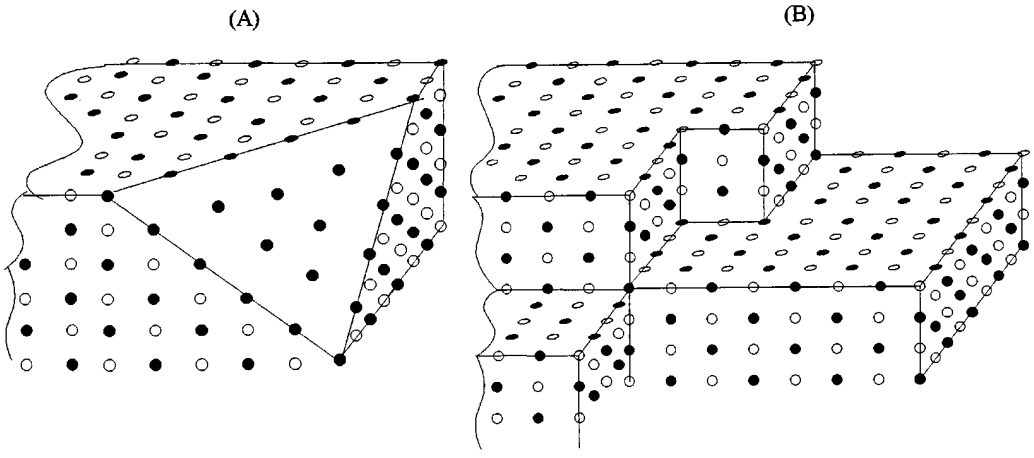

FIG. 7. Schematic representation of: (A) a terminating polar (111) surface plane of MgO and (B) (100) surface facets of MgO.

of MgO has in fact been reported previously by Moody and Warble (18) who suggested that adsorbed −OH groups on the terminating cations could infer extra stability to this surface. However, such −OH species have been shown by *in-situ* DRIFT experiments to be almost completely desorbed after calcination at 800°C on a sample maintained under Ar flow (9). Therefore, the actual dehydroxylated state of the MgO platelets calcined at 800°C should allow the surface to reconstruct to a series of {100}-type facets.

The intriguing observation that a sample which has been calcined at 800°C still retains a "(111) platelet morphology" suggests that the platelet surface may be stabilised by something other than adsorbed −OH groups. If an MgO crystallite is observed under nonaxial conditions at high magnifications, as in Fig. 8, it becomes possible to observe patches of a "disordered" phase on the platelet surface. EDX analysis (Table 2) and the strong mass contrast observed conform these regions to contain vanadium atoms. It is therefore demonstrated that the MgO (111) morphology is being stabilised up to 800°C by a thin V-containing surface overlayer. Under prolonged electron beam irradiation, the layer is seen to agglomerate into discrete patches. When this happens, the bare (111) surface becomes exposed and spontaneously reconstructs to a highly faceted {100}-type morphology as was previously noted in Figs. 5b, c.

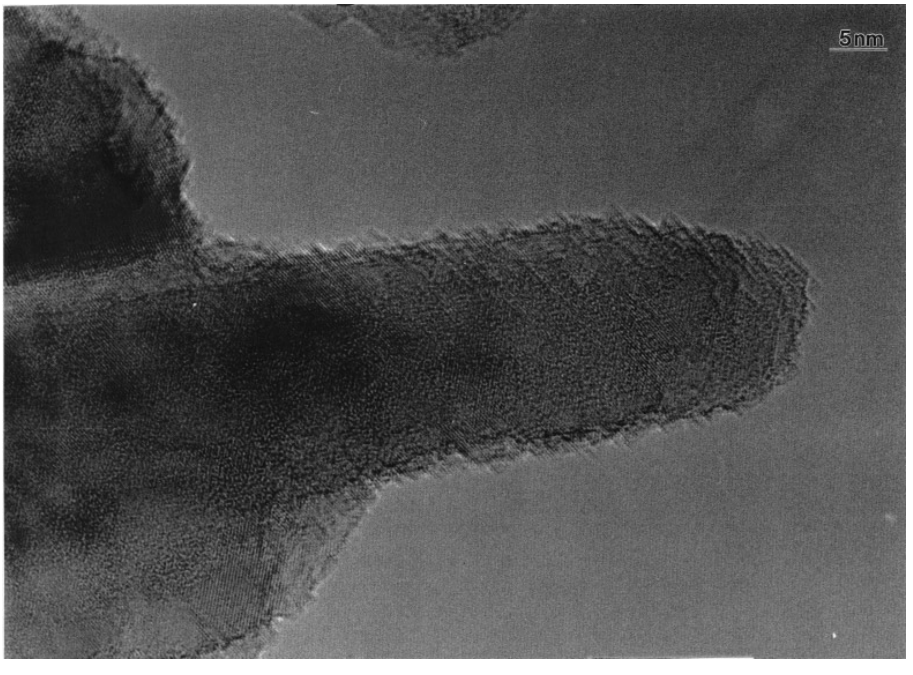

FIG. 8. High magnification micrograph of an MgO crystallite of the "FRESH" 14V/VMgO sample under nonaxial conditions.

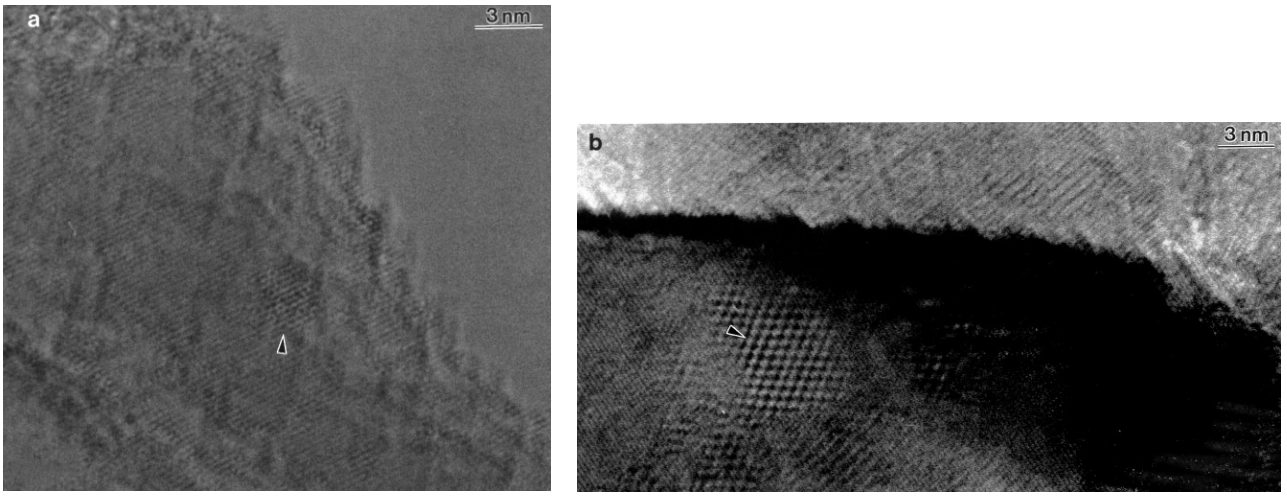

FIG. 9. High magnification micrographs of an MgO crystallite of the "USED" (a) and "USED-P" (b) 14V/VMgO sample.

3.3. State of the Active Surface after Catalytic Treatments

HREM analysis demonstrated that the MgO in the "USED" sample had still retained its (111) platelet morphology even after use (similar micrographs as the one related to the "FRESH" sample, depicted in Fig. 6). This implies that the V-containing stabilising overlayer remains intact during the catalytic reaction. However, detailed inspection of lattice fringe patterns indicates that the ODHP reaction has induced the overlayer to form a weakly ordered structure as shown in Fig. 9a (arrowed). The lattice fringe structure of the bulk orthovanadate and pyrovanadate phases (which are a minor fraction of the total catalyst volume) appeared to be relatively unaffected by the reaction.

Again, in the "USED-P" sample (reduced in a pure propane atmosphere) the same (111) MgO platelet morphology was found, but this time the particles were covered in a patchy fashion with a *strongly* ordered V-containing overlayer as shown in Fig. 9b. Furthermore, the fringe structure showed characteristic spacings and interplanar angles, suggesting that the overlayer has an epitaxial relationship with the MgO substrate. The fringe spacings and angles do not appear to match any projections of the bulk ortho-, pyro-, or metavanadate phases, nor the pure V_2O_5, V_2O_4, and V_2O_3 bulk phases. The fringes can, however, be fitted to a cubic MgV_2O_4 "spinel" type structure with lattice parameters of 8.4 Å. Details on this possibility are presented elsewhere (15).

On re-oxidation, the MgO [111] platelet morphology was retained and the thin film was observed to revert back to the disordered state similar in appearance to the "FRESH" sample shown in Fig. 8.

4. DISCUSSION

The *in-situ* electrical conductivity (Fig. 2) measurements showed unambiguously that the catalyst is reduced under typical reaction conditions and still more under a pure propane atmosphere by comparison with its state under oxygen atmosphere. These changes are completely reversible. A similar trend was indirectly observed by XPS, from the increase in the V^{4+}/V^{5+} atomic ratio after catalyst aging.

From the TEM-EDX study (Table 2), much of the exposed surface of the catalyst appears to be formed of small magnesia platelets with a vanadium-containing overlayer. This prominent phase of the catalyst will therefore be considered further on as the active surface. A strong crystallographic interaction is found to exist between this overlayer and the magnesia platelets. Electron microscopy showed that this vanadium-containing overlayer stabilises an unusual polar (111) orientation of MgO up to temperatures of 800°C. Furthermore, the HREM observations strongly suggest that an order/disorder transformation of this overlayer occurs in these materials, depending on the nature of the gaseous environment. Reduction of the catalyst with propane causes strong overlayer ordering, whereas oxidative treatments induce a transformation back to a disordered structure. Treatment in the propane/oxygen mixture, on the other hand, causes a less severe reduction and induces only a partial ordering of the overlayer.

UV-vis DR spectroscopy data (Fig. 3) complements the HREM-EDX data by indicating that the V overlayer on MgO crystallites is mainly formed of isolated and distorted (polymeric) V^{5+} tetrahedral units. The degree of V polymerisation is shown to slightly increase after ODHP reaction.

The above observations provide compelling evidence that a tight relationship exists between (i) the reducing/oxidising property of the surrounding atmosphere, (ii) the redox potential of the surface, and (iii) the degree of structural order of the vanadium-containing overlayer. All these phenomena are totally reversible.

Let us consider first the possible structure of the V^{5+} units supported on magnesia platelets which are found to be the main surface species of the 14V/VMgO optimised catalyst. The following characteristics have been associated with isolated tetrahedral V^{5+} species in vanadium-containing silicalite (19): (i) a stable tetrahedral environment, (ii) the presence of a V=O bond, (iii) the possibility of reversible reduction to a tetrahedral V^{4+} species, which can be reoxidised by gaseous oxygen via the formation of O activated species, (iv) the presence of strong Lewis acid sites after evacuation, and (v) the presence of V–O–Si stable bonds, which would limit the possibility of a nonselective O insertion. It was early suggested (3) that the presence of V=O bond would be rather detrimental to the ODH pathway at the expense of oxygen insertion process. In contrast, the presence of a V=O bond near a V–O bond was considered to further oxidise the propene towards combustion products (6). Note, however, that the combustion pathways also imply oxygen insertion processes.

The tetrahedral V^{5+} units revealed in the present study also present a character of isolated species in tight contact with the magnesia surface, therefore involving V–O–Mg bondings, able to stabilise the (111) orientation of MgO. However, these units can easily and reversibly polymerize and form precursors of spinel-like surface structure under reducing atmosphere. Such a behaviour, specific of the present catalyst, could be rationalized by assuming the following local coordination environment:

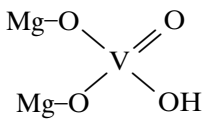

They would be isolated and/or corner linked units (as shown by UV spectroscopy) surrounded by anionic vacancies most likely related to the magnesia (as indicated by the electrical conductivity measurements).

Let us analyse now our results assuming the above surface units. A reducing atmosphere was shown to increase the surface ordering (Fig. 9). This appearance of local order could correspond to a polymerisation of isolated units, in accordance with the slight changes in the UV-vis. DR spectra after ODHP reaction (Fig. 3). Being reduced from V^{5+} to V^{4+} (or even to V^{3+} for a severe reduction possibly leading to the MgV_2O_4 structure (15)), V–O–V bondings are formed by sharing the double bonded oxygen atom between two neighboring V^{4+} atoms. The disappearance of V=O species (possibly responsible for total oxidation) upon surface reduction and ordering would explain the marked increase in selectivity towards propene formation in the absence of gaseous oxygen (observed during a transient period before catalyst deactivation, as reported in (10, 12)). Relating the polymerisation of isolated VO_4^{3-} units to surface ordering is quite consistent with the observation reported elsewhere (9) that the higher the total V content in the catalyst, the higher the fraction of the catalyst which crystallises as stoichiometric vanadate structures (ortho-, pyro-, then meta-vanadate). However, increasing the V content was also shown to unbalance the acid–base properties and to decrease the concentration of anionic vacancies required for a fast redox process. This corresponded to a marked decrease in the propene yield (9).

Now the question arises how to estimate the degree of MgO surface coverage by the amorphous VO_4^{3-} units. From structural calculations, the geometrical occupancy of VO_x units belonging to a monolayer of bidimensional polyvanadate was estimated to 0.1 nm^2/VO_x (20). By considering that the stabilised BET surface area reported in Table 1 (41 $m^2\ g^{-1}$) is essentially due to the dispersed magnesia phase (as clearly indicated by HREM), the theoretical surface concentration of VO_x units corresponding to a monolayer of polyvanadate can be directly evaluated as:

$$41 * 10^{18}(nm^2\ g^{-1})/0.1(nm^2/VO_x) = 410 * 10^{18}\ VO_x\ g^{-1}.$$

For the case of a monolayer of isolated monomeric units, the geometrical surface occupancy was estimated to 0.4 nm^2/VO_x (20). This gives a surface concentration of $102 * 10^{18}$ VO_x g^{-1} for a monolayer. By ignoring the few orthovanadate bulk crystallites detected by HREM and XRD, i.e., by considering that the 14V/VMgO catalyst is formed only of the V/MgO phase, the concentration of magnesium atoms is about $N/M_{MgO} = 6 * 10^{23}/40 = 15000 * 10^{18}$ Mg g^{-1}. From the EDX V/Mg atomic ratio pertaining to this V/magnesia phase (1/45 in Table 2), the effective concentration of V units dispersed over the magnesia can then be estimated to $15000 * 10^{18}/45 = 333 * 10^{18}$ VO_x g^{-1}. Indeed, this value must be considered as an upper limit of the real concentration, within the above assumptions and uncertainties involved in the calculation. However, it clearly indicates that the actual magnesia coverage by the V units is below a monolayer of bidimensional polyvanadate (in accordance with Wachs *et al.* (20)), but is larger than a monolayer of isolated monomers. The most likely state of the V-containing overlayer is therefore a monolayer of mixed isolated and polymeric species, as clearly indicated by the UV-vis DR spectroscopy. A rough quantitative evaluation based on the above figures gives 25 and 75% of isolated and polymeric V^{5+} units, respectively, which may satisfactorily account for the profile of the UV-vis DR spectra reported in Fig. 3.

The second key information of the present study is that the surface reduction under reducing conditions (ODHP reaction or a pure propane atmosphere) and the subsequent surface ordering are found to correlate with a significant increase in the electrical conductivity of the catalysts. The *n*-type electrical conductivity is shown to be related, at least partly, to doubly ionised anionic vacancies (□). In this respect, the increase of the electrical conductivity

upon catalyst reduction can be accounted for by assuming that the electrons arising from the V^{5+} to V^{4+} (or even to V^{3+}) reduction become available for the surface conductivity and vice versa after catalyst reoxidation. This redox process can be directly related to the propane-to-propene dehydrogenation step as

$$C_3H_8 + 2\{V^{5+} + \square + O^{2-}\} \rightarrow C_3H_6 + 2\{V^{4+} + \square\} + 2OH^- \quad [1]$$

and to the dehydroxylation/reoxidation steps as

$$2OH^- \rightarrow H_2O + O^{2-} + \square \quad [2]$$

$$2\{V^{4+} + \square\} + \frac{1}{2}O_2 \rightarrow 2V^{5+} + \square + O^{2-}. \quad [3]$$

5. CONCLUSION

At variance with literature proposals assuming that specific VMgO phases are solely responsible for the selective dehydrogenation of propane (3, 4) the present study revealed that much of the exposed surface of the catalyst consists of dispersed vanadia surface units having intimate crystallographic interaction with magnesia crystallites. These surface vanadia units form a monolayer of both monomeric and polymeric species, which stabilise an unusual polar (111) orientation of MgO up to temperatures of 800°C. The outstanding discovery was the direct observation of a totally reversible phenomenon of order/disorder restructuration of this V overlayer in conjunction with the redox state of the surface depending on the characteristics (reductive or oxidative) of the surrounding atmosphere. These fast surface phenomena are assumed to determine the elementary steps of propane activation within the overall ODHP process.

ACKNOWLEDGMENTS

Financial support from the EU HCM network "Euroxycat" and the JOULE programme Contract JOE 3CT950022 is gratefully acknowledged. Thanks are due to Drs. J. M. Herrmann, G. Bergeret, J. Perregaard, and P. E. Højlund Nielsen for fruitful discussions.

REFERENCES

1. Somorjai, G., "Introduction to Surface Chemistry and Catalysis," Wiley, New York, 1994.
2. Topsoe, H., Ovesen, C. V., Clausen, B. S., Topsoe, N.-Y., Højlund, Nielsen, Törnqvist, E., and Nørskov, J. K., "Dynamics of Surface and Reaction Kinetics in Heterogeneous Catalysis" (G. F. Froment *et al.*, Eds.), Studies in Surface Science and Catalysis, Vol. 109, p. 121. Elsevier, Amsterdam, 1997.
3. Chaar, M. A., Patel, D., and Kung, H. H., *J. Catal.* **109**, 463 (1988).
4. Siew Hew Sam, D., Soenen, V., and Volta, J. C., *J. Catal.* **123**, 417 (1990).
5. Michalakos, P. M., Kung, M. C., Jahan, I., and Kung, H. H., *J. Catal.* **140**, 226 (1993).
6. Corma, A., López Nieto, J. M., and Paredes, N., *J. Catal.* **144**, 425 (1993). [*Appl. Catal.* **104**, 161 (1993).]
7. Kung, H. H., and Kung, M. C., *Appl. Catal. A* **157**, 105 (1997).
8. Gao, X., Ruiz, P., Xin, Q., Guo, X., and Delmon, B., *J. Catal.* **148**, 56 (1994).
9. Pantazidis, A., and Mirodatos, C., "Heterogeneous Hydrocarbon Oxidation" (B. Warren and S. T. Oyama, Ed.), ACS Symposium Series, Vol. 638, p. 207. Am. Chem. Soc., Washington, DC, 1996.
10. Pantazidis, A., Auroux, A., Herrmann, J.-M., and Mirodatos, C., *Catal. Today* **32**, 81 (1996).
11. Pantazidis, A., and Mirodatos, C., *in* "11th International Congress on Catalysis" (J. W. Hightower, W. N. Delglass, E. Iglesia, and A. T. Bell, Eds.), Studies in Surface Science and Catalysis, Vol. 101, p. 1029. Elsevier, Amsterdam, 1996.
12. Pantazidis, A., Forissier, M., and Mirodatos, C., in preparation.
13. Herrmann, J. M., Applications of Electrical Conductivity Measurements in Heterogeneous Catalysis, *in* "Catalyst Characterization" (B. Imelik and J. C. Vedrine, Eds.). Plenum, New York, 1994.
14. Briggs, D., and Seath, M. P. (Eds.), "Practical Surface Analysis, Auger and X-ray Photoelectron Spectroscopy," p. 1. Wiley, Chichester, 1990.
15. Burrows, A., Kiely, C. J., Perregaard, J., Vorbeck, G., Törnqvist, E., and Højlund-Nielsen, P. E., in preparation.
16. Hanuza, J., Jezowska-Trzebiatowska, B., and Oganowski, W., *J. Mol. Catal.* **29**, 109 (1985).
17. Burrows, A., Kiely, C. J., Pantazidis, A., Mirodatos, C., and Derouane, E. G., *Catal. Lett.*, in preparation.
18. Moody, A. F., and Warble, C. E., *J. Cryst. Growth* **10**, 26 (1971).
19. Bellussi, G., Centi, G., Perathoner, S., and Trifiro, F., *in* "Catalytic Selective Oxidation" (S. T. Oyama and J. W. Hightower, Eds.). ACS Symposium Series, Vol. 523, p. 281. Am. Chem. Soc., Washington, DC, 1993.
20. Wachs, I. E., and Weckhuysen, B. M., *Appl. Catal. A* **157**, 67 (1997).